

Research Article

Nanoceria Decrease Vascular Permeability in a Mouse Model of AMD

Cai X^{1*}, Seal S⁴ and McGinnis JF^{1,2,3*}¹Department of Ophthalmology, University of Oklahoma Health Sciences Center, USA²Department of Cell Biology and Oklahoma Center for Neuroscience, University of Oklahoma Health Sciences Center, USA³Department of Oklahoma Center for Neuroscience, University of Oklahoma Health Sciences Center, USA⁴Advanced Materials Processing Analysis Center, University of Central Florida, USA

*Corresponding authors: Xue Cai, Department of Ophthalmology, University of Oklahoma Health Sciences Center, 608 Stanton L. Young Blvd, Oklahoma City, OK 73104, USA

McGinnis JF, Department of Ophthalmology, University of Oklahoma Health Sciences Center, 608 Stanton L. Young Blvd, Oklahoma City, OK 73104, USA

Received: September 22, 2016; Accepted: October 25, 2016; Published: October 27, 2016

Abstract

The Very Low Density Lipoprotein Receptor Knockout (*vldlr*^{-/-}) mouse is a model for a distinct form of Age-Related Macular Degeneration (AMD) called Retinal Angiomatous Proliferation (RAP). It is characterized by neovascularization, increased vascular permeability and retinal degeneration. We have reported that administration of nanoceria to pigmented *vldlr*^{-/-} mice significantly inhibits the developmental neovascularization when injected at postnatal day (P) 7 and produces sustained regression of the existing neovascularization when applied at P28. In this study, we characterized the effects of the homozygous presence of the *vldlr* mutation on an albino background on retinal degeneration and neovascularization. We also examined the effects of increasing concentrations of nanoceria on: inhibition of the expression of Vascular Epithelium Growth Factor (VEGF), the number of retinal and choroidal neovascularization, the health of Retinal Pigment Epithelium (RPE) cells and the loss of RPE junctional proteins using albino *vldlr*^{-/-} mice. Our data demonstrate that nanoceria function in a dose-dependent manner to up-regulate the expression of RPE65 and tight-junction proteins, down-regulate angiogenesis-stimulating factors, inhibit Blood-Retinal Barrier (BRB) breakdown and decrease vascular permeability in adult mice. These findings suggest that nanoceria are potential therapeutics for treatment of ocular diseases caused by RPE dystrophy and BRB dysfunction.

Keywords: Albino *vldlr*^{-/-} mice; Nanoceria; RPE; Tight-junction proteins; Blood-retinal barrier

Abbreviations

AMD: Age-Related Macular Degeneration; BRB: Outer Blood-Retinal Barrier; CNV: Choroidal Neovascular “tufts”; FITC: Fluorescein Isothiocyanate; INL: Inner Nuclear Layer; Nanoceria: Cerium Oxide Nanoparticles; ONL: Outer Nuclear Layer; OPL: Outer Plexiform Layer; qRT-PCR: Quantitative Real Time RT-PCR; RAP: Retinal Angiomatous Proliferation; RNV: Retinal Neovascular “blebs”; ROS: Reactive Oxygen Species; RPE: Retinal Pigment Epithelium; TRX: Thioredoxin; VEGF: Vascular Epithelium Growth Factor; *vldlr*^{-/-}: Very Low Density Lipoprotein Receptor Knockout; wt: Wild Type; ZO: Zonula Occludens

Introduction

The Retinal Pigment Epithelium (RPE) cells form a monolayer of cells in the back of the eye adjacent to the photoreceptors and play important physiological and functional roles in the process of conversion of light to neural signals [1,2]. The communication and cooperation between RPE cells and photoreceptors completes the visual cycle. The RPE cells, which contain pigmented granules, shield the photoreceptors from excessive light, and digest the aged outer segment discs of photoreceptors. The RPE cell also secretes growth factors, transports nutrients and provides iron channels [2]. It forms an outer Blood-Retinal Barrier (BRB) to control vascular fluid (as well as to absorb fluid from the retinal space) and exchanges nutrients and metabolic materials between the choroid and subretinal space [1]. This enables it to be highly selective in the modulation of the movement of oxygen and other molecules from the choroidal circulation system

to the retina [3,4]. The tight junction complex forms the fundamental structure of the BRB and contributes to epithelial cell adhesion, communication and cellular movement. More than 40 proteins are found to be closely associated with tight junctions [5]. Among them, transmembrane claudins and occludin, and the scaffolding Zonula Occludens (ZO) proteins play essential roles in the formation and regulation of the BRB.

Breakdown of the BRB and consequences of the dysregulation of vascular permeability are closely associated with angiogenesis and can result in retinal edema [6-8]. This pathological condition is also correlated with an elevation of Vascular Epithelium Growth Factor (VEGF) [9,10]. The progression of the pathology of Age-Related Macular Degeneration (AMD) is predominantly and strongly correlated with oxidative stress-induced molecular and cellular injury, and the deposition of damaged proteins and other molecules in the RPE cells results in dystrophy of the RPE [11,12]. The central role of the RPE cell and the correlation of its dysfunction with the pathogenesis of AMD have been demonstrated by many laboratories [13,14]. The eventual degeneration of photoreceptors appears to be secondary to RPE senescence [15].

We have previously shown that catalytic inorganic Cerium Oxide Nanoparticles (nanoceria), which regeneratively scavenge Reactive Oxygen Species (ROS) and mimic the activities of the antioxidative enzymes, superoxide dismutase and catalase [16-18], have therapeutic effects against light-induced damage to the retina of albino Wild Type (wt) rats [19]. We have also shown that nanoceria prevent retinal degeneration in *tubby* mice [20,21] and inhibit the development

of neovascularization and cause regression of the existing neovascularization in pigmented *vldlr*^{-/-} mice [22,23]. Recently, we demonstrated that long-term retention of nanoceria in the retina does not induce any changes in retinal structure and function in albino rats [24], and we did not detect any increased inflammatory responses caused by any of the nanoceria concentrations tested in wt mice [25]. In the current study, we focus on the ability of nanoceria to provide protection to RPE cells, regulate tight-junctions and other junctional proteins, and to inhibit increased vascular permeability in adult albino *vldlr*^{-/-} mice.

Materials and Methods

Intravitreal injection

Saline (1 μ l), or saline with increasing concentrations of nanoceria from 0.001 mM (0.172 ng), 0.01 mM (1.72 ng), 0.1 mM (17.2 ng), 1 mM (172 ng) to 10 mM (1720 ng) were delivered into the vitreous of the albino *vldlr*^{-/-} mice at P28 by injection as previously reported [23]. Uninjected *vldlr*^{-/-} and wt Balb/C mice served as controls.

Vascular filling assay

The mice, at scheduled time points, were anesthetized and then 40 μ l of 2.5% high molecular weight Fluorescein Isothiocyanate (FITC) - dextran (Sigma-Aldrich, FD-2000S) were injected into the left ventricle of the heart [22,23]. The anesthetized mice were killed 5 minutes later; the eyes were enucleated and fixed in 4% paraformaldehyde. The eyes were dissected, flat-mounted, observed and imaged as previously reported [22,23]. Eyes (20-30 per group) were analyzed and retinal neovascular "blebs" and choroidal neovascular "tufts" were counted using an Olympus MVX10 stereomicroscope. Data shown are mean \pm SEM.

Fundus imaging and fluorescein angiography

Observation of the fundus and neovascularization were done as previously reported [23] with minor modification. Briefly, mice were anesthetized, the eyes were dilated, and the mice were placed on the bed of the Micron III system (Phoenix Research Labs, Pleasanton, CA). After the fundus was clearly seen and images taken, 20 μ l of 5% AK-Fluor (Alcon) was intraperitoneally injected into the mouse. The photographs were captured 30 seconds, 60 seconds and 90 seconds after injection using StreamPix software and blue filters.

Optical Coherence Tomography (OCT)

Mice were fully anesthetized and eyes were dilated. One drop of refresh optive moisturizing solution was placed on the cornea. The mouse was put on the adjustable curset of the OCT machine (Bioptigen) and the head was held in a proper position, then the retina was scanned and images were saved.

Electroretinography (ERG)

Mice were dark adapted overnight, the eyes were dilated, and intensity scotopic ERGs were performed at P35 days with light intensities of 0.002, 0.02, 0.2, 2, 200 and 2000 cds /m². Full field scotopic ERG with light intensity of 600 cds /m² and photopic ERG with light intensity of 1000 cds /m² were performed at P35 days (P35d), 3 months (P3m), and 7 months (P7m).

Immunocytochemistry and whole mount immunofluorescence staining

The eyes were collected, fixed, dissected as eyecups (SCR,

Sclera-Choroid-RPE) without lens and cornea. For flat mount immunofluorescence staining, the dissected SCRs were blocked with 5% BSA, incubated with primary antibodies: either mouse anti-RPE65 (1:500, Millipore) or rabbit anti-ZO-1 (1:300, invitrogen) at 4°C overnight then incubated in anti-mouse or anti-rabbit AlexaFluor 488 for 1 hr at room temperature. After DAPI counterstaining, the SCRs were flat-mounted on the slides with RPE face-up and 4-6 radial cuts were made before coverslipping. For cryosectioning, the SCRs were embedded in OCT media and 10 μ m sections were cut as previously reported [20,23]. The slide-mounted cryo-sections were blocked and incubated in the above primary antibodies at room temperature for 2 hrs, then incubated in anti-mouse or anti-rabbit AlexaFluor 488 for 1 hr at room temperature. After DAPI counterstaining the slides were coverslipped. Image capture was performed using a Nikon Eclipse 800 epi-fluorescence microscope.

Histology and quantitation of nuclei

The procedure for histology is the same as previously reported [20,23]. H & E stained slides from eyes at different developmental stages were observed and imaged with a Nikon Eclipse 800 microscope under 10x and 40x. For morphometry and quantitative histological analysis, three fields with 0.48 mm intervals between each field were imaged superiorly and inferiorly under 40x with the first image at a distance of 0.48 mm from ONH (Optic Nerve Head). The number of nuclei in the Outer Nuclear Layer (ONL) was determined (3-6 eyes per group) and the data shown are the averages of all measurements within the same age per group.

Quantitative Real Time RT-PCR (qRT-PCR)

Eyecups (3-5), without cornea and lens, from each group at P35 days, were collected and kept in TRIzol at -80°C. Total RNA isolation and cDNA synthesis are the same as previously reported [20]. For each sample, 20 ng of cDNA in triplicate was used for qRT-PCR reactions to determine the mRNA levels of VEGF. Primer sequences for the VEGF gene and the house-keeping gene (GAPDH) are the same as previously reported [23]. Relative expression levels were calculated [23] and are shown as mean \pm SEM.

Western blot

Eyecups (3-8) from each group were collected. Protein extraction, quantitation, gel electrophoreses, membrane transfer and membrane development were the same as previously reported [20]. Soluble protein (50 μ g) was loaded in each well of the gel. The following primary antibodies were used: sheep anti-VEGF and goat anti-Occludin (1:1000 and 1:750 respectively, Santa Cruz), mouse anti-RPE65 (1:2000, Millipore), anti-IL-1 β (1:1000, Millipore), rabbit anti-ZO-1 (1:500, invitrogen), anti-TNF- α (1:1000, Millipore), and anti-IL-6 (1:1000, Proteintech). Rabbit anti- β -actin (HRP conjugate) (1:1000, cell signaling technology) or anti-GAPDH (1:2500, Abcam) antibody served as loading controls. The band detection and densitometric analysis of the bands were performed as previously reported [20,23].

Statistical analysis

One way ANOVA analysis with Bonferroni post hoc test and/or unpaired student *t*-test was performed and *P* value of less than 0.05 (*P*<0.05) was considered as a significant difference and is indicated in each figure.

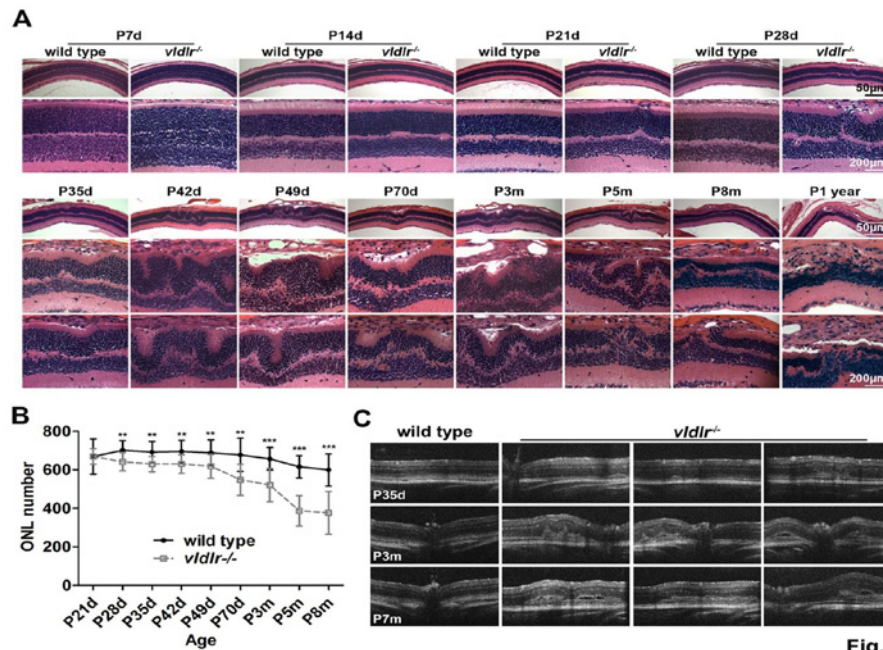


Fig. 1

Figure 1: Neovascularization and retinal structure changes occur over time in the *vldlr*^{-/-} retinas. (A) The neovascularization arises from the OPL and disruptions of retinal structure begin to be seen at P21 days. Thereafter, abnormal retinal structures are seen throughout the retina. Representative images from each group are shown. N=3-6 eyes per group. Scale bar, 50 μ m and 200 μ m, respectively. (B) Quantitation of nuclei in the ONL demonstrates temporal loss of photoreceptor cells in *vldlr*^{-/-} mice. The number of nuclei from 3-6 eyes with 18-36 measurements per group of mice was determined at each of the time points listed. ** $P < 0.0003$, *** $P < 0.000001$. (C) OCT reveals the progression of the neovascularization development in *vldlr*^{-/-} mice. Compared to wt, the enlargement and fusion of the neovascularization, retinal thickening, and eventual retinal detachment occur in the mutant mice. Representative OCT images from each group are shown. N=5-8 eyes per group.

Results

Retinal development and photoreceptor degeneration in albino *vldlr*^{-/-} mice

Eyes at P7–365 were collected and processed for analysis of the development of the retina and neovascularization. There are no major differences in retinal morphology and the nuclear number in the ONL of albino *vldlr*^{-/-} and wt Balb/C mice at P7 and P14 (Figure 1A) although the initiation of neovascularization in *vldlr*^{-/-} mice occasionally appeared at P14. The obvious retinal structural changes, because of the penetration of neo-blood vessels from the Outer Plexiform Layer (OPL) through the ONL and connecting to the choroid, were always seen at P21 (Figure 1A). Histological analysis indicated that the mutant retinas at P28 have 91.39% of the nuclei present in age-matched wt littermates (Figure 1B). Severe ONL abnormalities with regional increases in RPE layers, accompanied by photoreceptor cell death (Figure 1A, Figure 1B), are frequently observed after P35. At P49, retinal detachment occurred because of drusen formation (Figure 1A), and at P70, about 20% of the photoreceptors were lost. Severe retinal degeneration occurred by P5m, when 37% of photoreceptor cells in the mutant retinas were absent (Figure 1B). Irregular retinal structures, such as a thickened RPE with multiple layers of cells, rosette-like structures in the ONL, thinning of the ONL and/or INL (Inner Nuclear Layer) beneath the lesion area, and the fusion of the retinal neovascular vessels and choroidal neovascular vessels represent the typical retinal morphology in *vldlr*^{-/-} mice (Figure 1A). OCT images of the retina of living *vldlr*^{-/-} mice at P35d, P3m and P7m revealed the progressive development of

the lesions, the enlarged fused neovascularization, and retinal thickening indicative of edema, all of which eventually cause severe retinal detachment (Figure 1C). To further examine the retinal degeneration and its function in response to light, full field ERG (Figure 2A) was performed at P35d, P3m and P7m of age. The amplitude of cone ERG at P35d had decreased to 71.5% of wt and it further decreased to 61% of wt by P7m. In contrast, the rod function has no large changes at P35d when measured by full field ERG. However, intensity ERG (Figure 2B) at P35d demonstrated that the rod sensitivity to light in *vldlr*^{-/-} mice is statistically lower than in wt mice. Rod response to the light in *vldlr*^{-/-} mice declined to 76% of wt at P3m (a-wave only, the b-wave has minor changes) and it was only 69% of wt at P7m (Figure 2A). These data indicate that cone degeneration occurred earlier than rod degeneration and degeneration of secondary neurons occurs later than the primary neurons.

Neovascularization development and leakage in albino *vldlr*^{-/-} mice

Initial formation of abnormal blood vessels was seen at P14 and originated from the inner retina and progressed towards the subretinal space (Figure 1A). Abnormal retinal structure was evident at P21 (Figure 1A), and using an FITC-Dextran vascular filling assay (Figure 3A), numerous Retinal Neovascular “blebs” (RNV) can be seen at this time. However, a few typical choroidal “neo” vessels can also be seen in some of the eyes at this age (Figure 3A). Significant increases in the number of Choroidal Neovascular “tufts” (CNV) occurred by P28. Both blebs and tufts reached the maximum number at P35, an age earlier than in the pigmented *vldlr*^{-/-} mice in which

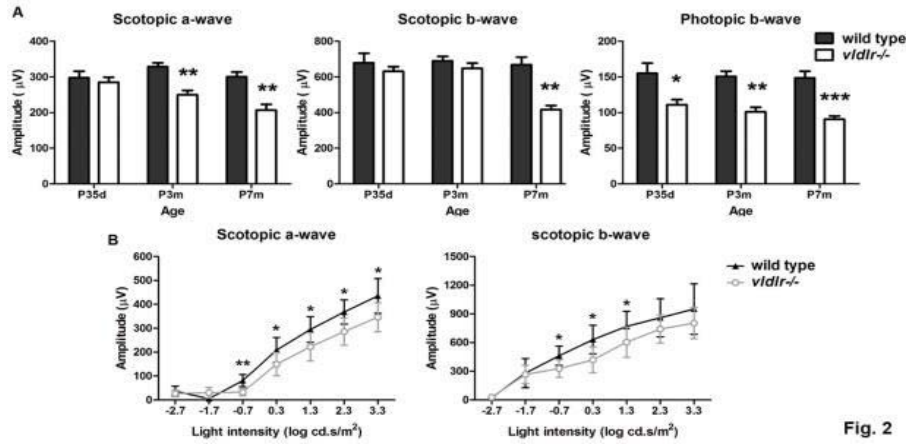


Fig. 2

Figure 2: Electretinography demonstrates losses in retinal function over time in *vldlr*^{-/-} mice. (A) Full field ERG evaluation of retinal function shows that cone function declines, but rod function is similar to wt at P35d. Reduced rod function was detected at P3m in *vldlr*^{-/-} mice and intensity ERG evaluation at P35d (B) demonstrated that the rod function has actually declined in mutant mice. N=7-14 animals, *P<0.05, **P<0.005, ***P<0.0001.

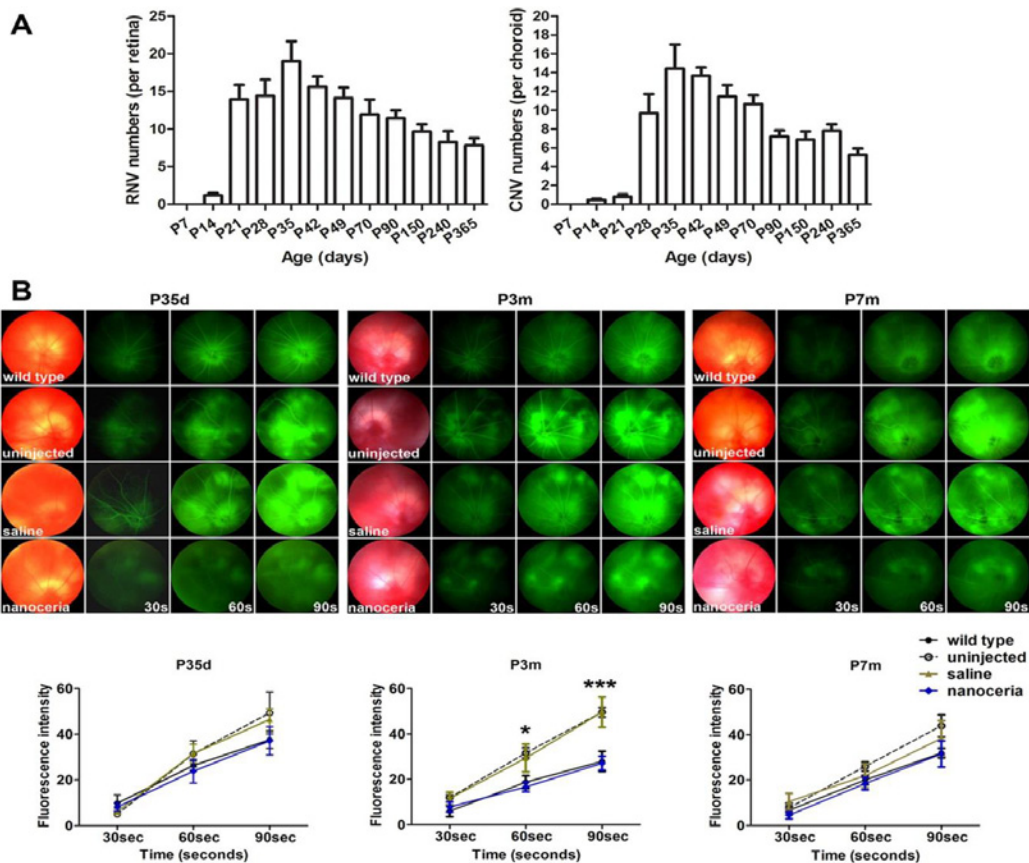


Fig. 3

Figure 3: Nanoceria inhibit neovascularization and vascular leakage. (A) Vascular filling assays over a one year period indicated that the number of Retinal Neovascular “blebs” (RNV) greatly increased by P21d and the number of Choroidal Neovascular “tufts” (CNV) greatly increased by P28d. Both RNV and CNV reached their highest numbers by P35d. N=10-30 eyes per group. (B) Fundoscopy and fluorescein angiography (top) at P35d, P3m and P7m demonstrated that, the fluorescein intensity is greatly increased in the mutant over time compared to the wt controls demonstrating the increased vascular permeability, whereas nanoceria treatment considerably decreased the fluorescein leakage. Quantitation of fluorescein intensity (bottom) at the above time points supports that conclusion. N=5-8 eyes per group, *P<0.05, ***P<0.001.

maximum neovascularization occurred at P42 [26]. In addition, the vascular filling assay also showed that the number of RNV and

CNV in albino *vldlr*^{-/-} mice is much less than that in the pigmented *vldlr*^{-/-} mice [22] (Figure 3A). Fundoscopic imaging and fluorescein

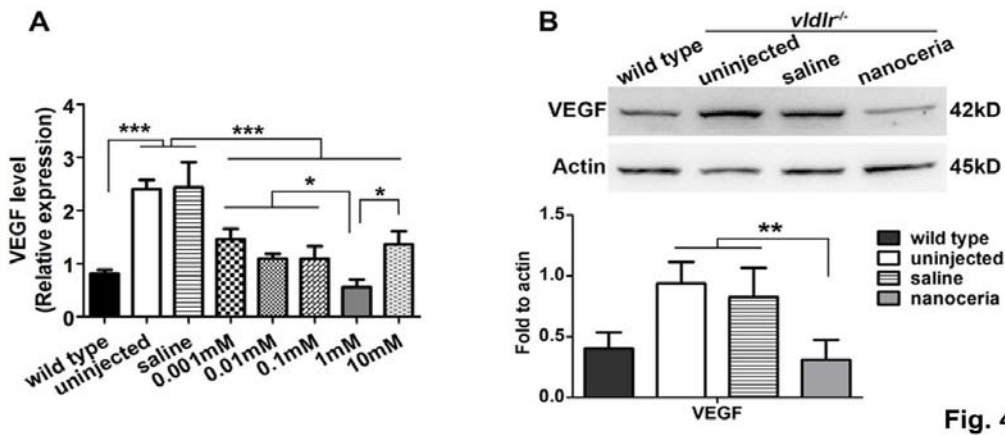


Fig. 4

Figure 4: Nanoceria decrease VEGF expression in a dose dependent manner. (A) qRT-PCR analysis at P35 demonstrated that the elevated VEGF mRNA expression in *vldlr*^{-/-} retinas was progressively decreased with increasing amounts of nanoceria with 1mM having the highest effect. N=3-5 eyes per group. *P<0.05, ***P<0.0001. (B) Western blot and densitometric analysis of the bands demonstrated that VEGF levels in uninjected and saline injected *vldlr*^{-/-} eyes are more than 2 fold higher than in wt. Treatment with 1 mM nanoceria reduced the VEGF level to the equivalent of wt. N=3-8 eyes per group. **P<0.005.

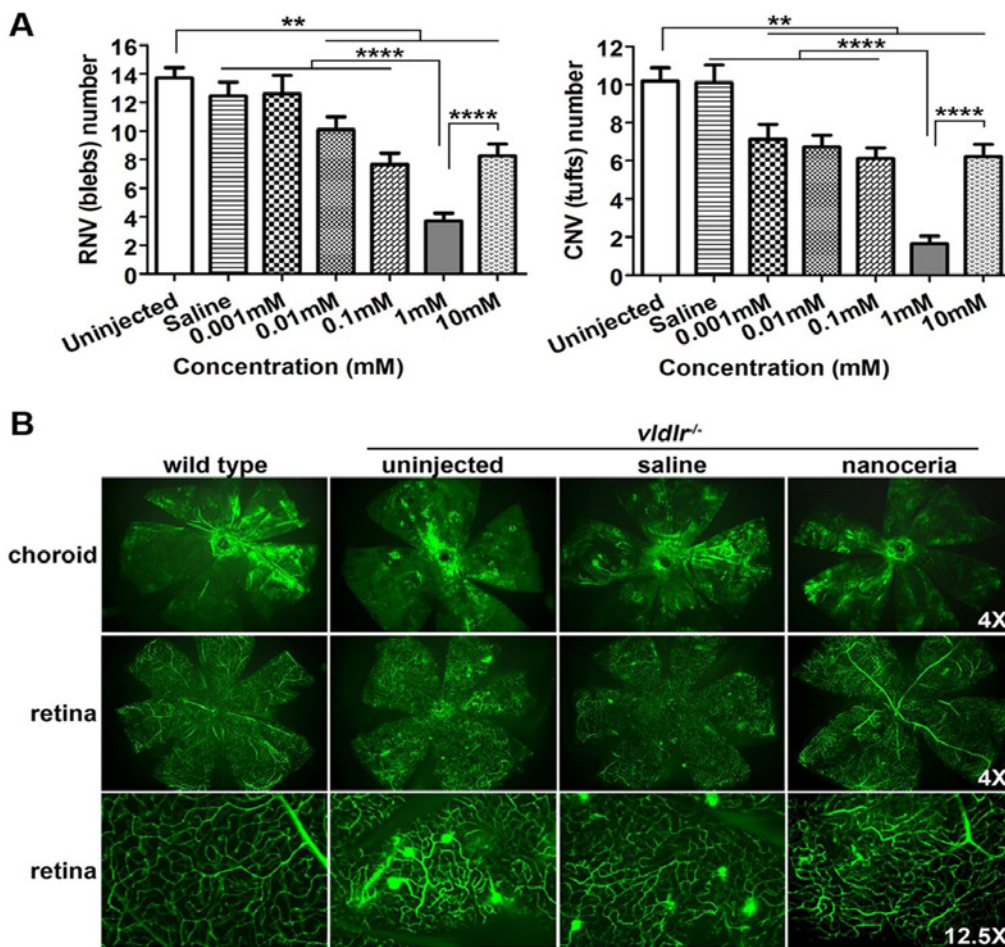


Fig. 5

Figure 5: Nanoceria inhibit neovascularization in a dose dependent manner. (A) Quantitation of RNV and CNV number. (B) Representative eyes of vascular filling assay from each group are shown. N=10-20 eyes per group. **P<0.005, ****P<0.00001.

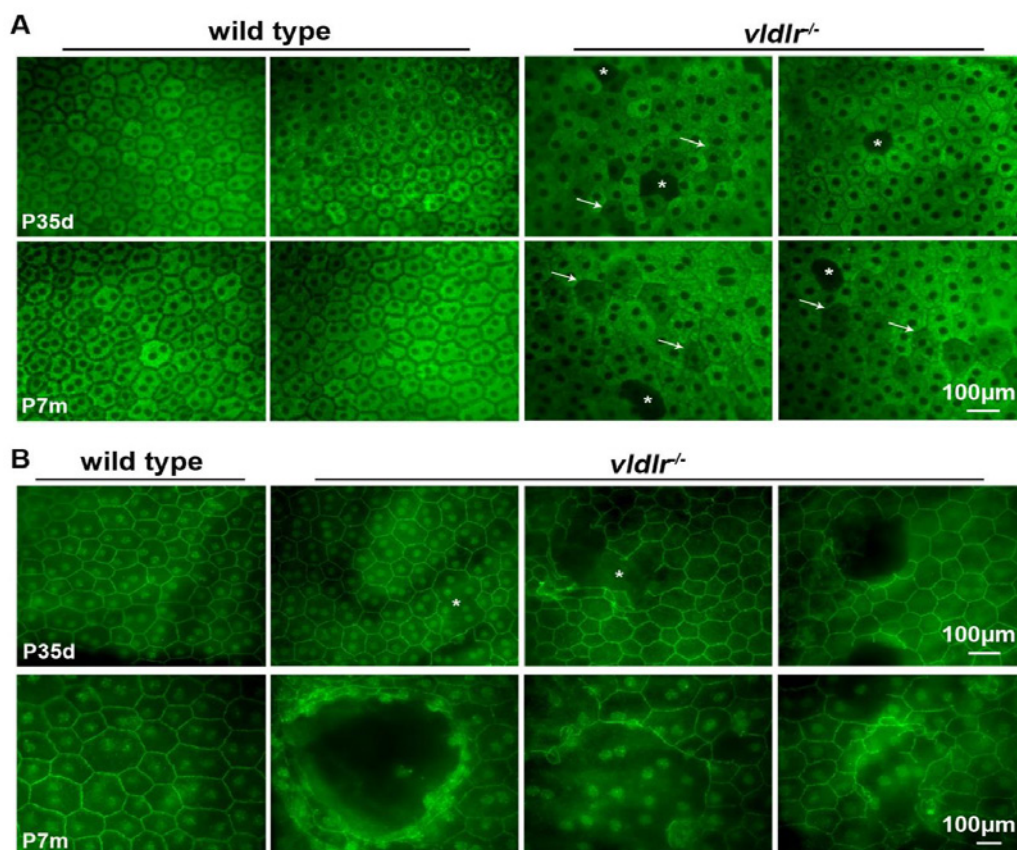


Fig. 6

Figure 6: Whole mount immunostaining of eye cups indicates that RPE65 and ZO-1 in *vldlr*^{-/-} mutants are decreased. (A) Weaker RPE65 fluorescence (arrow) and fluorescence voids (asterisk) were seen in the mutant mice compared to the strong fluorescence in the wt. (B) Junctional integrity of ZO-1 is seen in the solid narrow boundary of the RPE cells in wt, whereas the expression pattern in the mutant is disrupted and discontinuous (asterisk). N=10-12 eyes per group. Scale bar, 100 μm.

angiography demonstrated the neovascularization in the retina of the albino *vldlr*^{-/-} mice as bright spots from which severe fluorescein leakage (Figure 3B) occurred. *In vivo* evaluation of the time course of fluorescein intensity at P35d, P3m and P7m (Figure 3B) showed that the uninjected and saline injected *vldlr*^{-/-} mice progressively exhibited more severe leakage of fluorescein dye with increasing time, compared to the wt. Nanoceria treatment inhibited the leakage and decreased the fluorescence intensity level similar to that seen in the wt (Figure 3B).

Nanoceria function in a dose-dependent manner

We next examined the effects of different doses of nanoceria. 1 μl of increasing concentrations of nanoceria (0.001 mM, 0.01 mM, 0.1 mM, 1 mM and 10 mM) was intravitreally injected at P28, and then the transcription level of VEGF, and the number of RNV and CNV was evaluated at P35 by qRT-PCR (Figure 4) and an FITC-dextran vascular filling assay (Figure 5A). The data demonstrated that nanoceria at 0.001 mM reduced VEGF expression by 1.30 and 1.34 fold of the levels found in uninjected and saline injected *vldlr*^{-/-} mice, respectively. The VEGF levels were further decreased with increasing nanoceria doses. The highest inhibition of VEGF expression was reached with 1 mM nanoceria, which significantly decreased VEGF more than 3 fold compared to the uninjected (P=0.003092) and saline

injected mice (P=0.011325). However, inhibition of VEGF expression by nanoceria at 10 mM is not significantly different from that seen with 0.001 mM (P=0.480162) (Figure 4A). Western blots, to analyze the expression of VEGF protein at P35, demonstrated that VEGF was increased in mutant mice and was down regulated by treatment with 1 mM nanoceria (Figure 4B). Moreover, quantification of vascular filling assays showed that the number of RNV and CNV was progressively reduced with increasing concentrations of nanoceria. However the number of RNV and CNV in the eyes injected with 10 mM of nanoceria was similar to that seen with 0.1 mM concentration (Figure 5B). Our data further support the conclusion of our previous report that 1 μl of 1 mM nanoceria provides the maximum effect in cultured cells and mouse tissues [27].

Nanoceria up regulate RPE65 and the junctional proteins

Next we determined the expression, localization and distribution of an RPE specific protein and the proteins of the junctional complex in *vldlr*^{-/-} RPE cells. Immunofluorescent labeling of RPE65 in whole mount eyecups (Figure 6A) at P35d shows uniform intensity of fluorescence in RPE cells in the wt mice but variable intensities in *vldlr*^{-/-} RPE cells, with some cells being completely devoid of fluorescence. Many more RPE cells have very weak RPE65 labeling at P7 months. ZO-1 protein distribution (Figure 6B) in the boundary of the cells

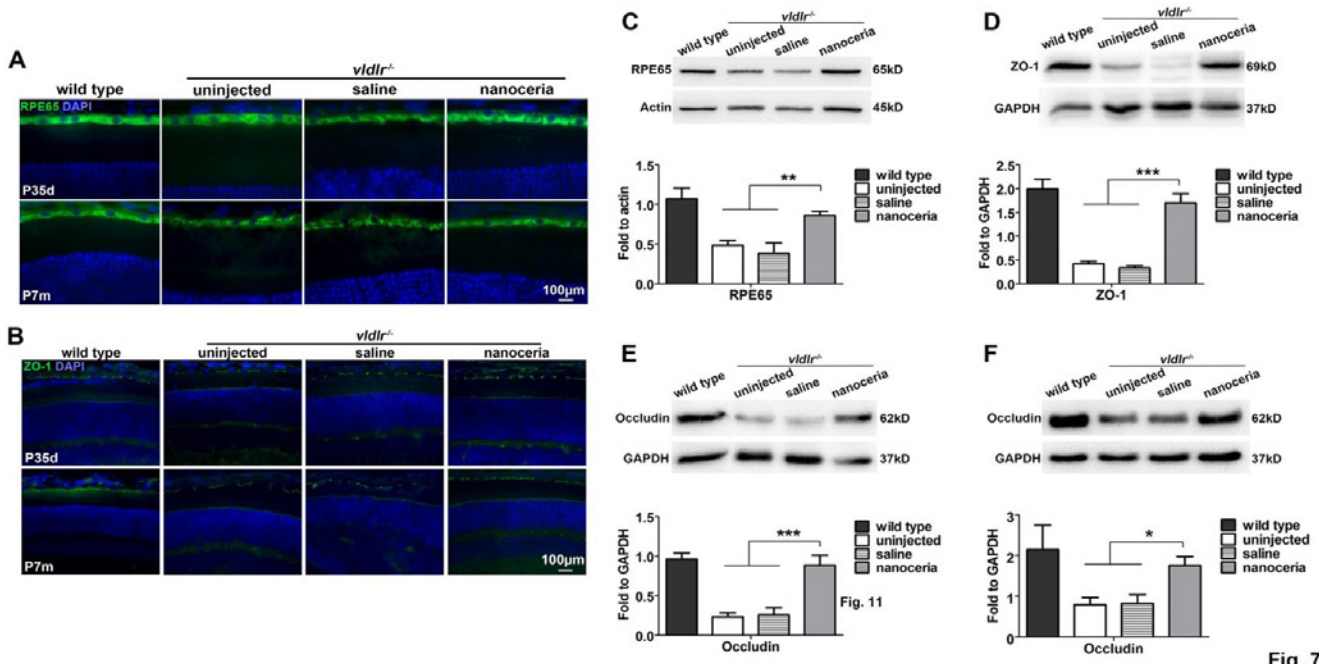


Fig. 7

Figure 7: Nanoceria increase the expression and improve the distribution of RPE65 and junctional proteins. Immunostaining of RPE65 (A) and ZO-1 (B) in cryosections at P35d and P7m showed that nanoceria treatment increased the distribution and fluorescence intensity of these two proteins. N=5-8 eyes per group. Scale bar, 100 μm. (C-F) Western blot assay showed that the protein levels of RPE65 (C), ZO-1 (D), and Occludin (E, F) are greatly decreased in the mutant, and nanoceria treatment significantly increased their levels. (C), (D) and (E) are at P35d, (F) is at P7m. N=5-7 eyes per group. *P<0.05, **P<0.001, ***P<0.0001.

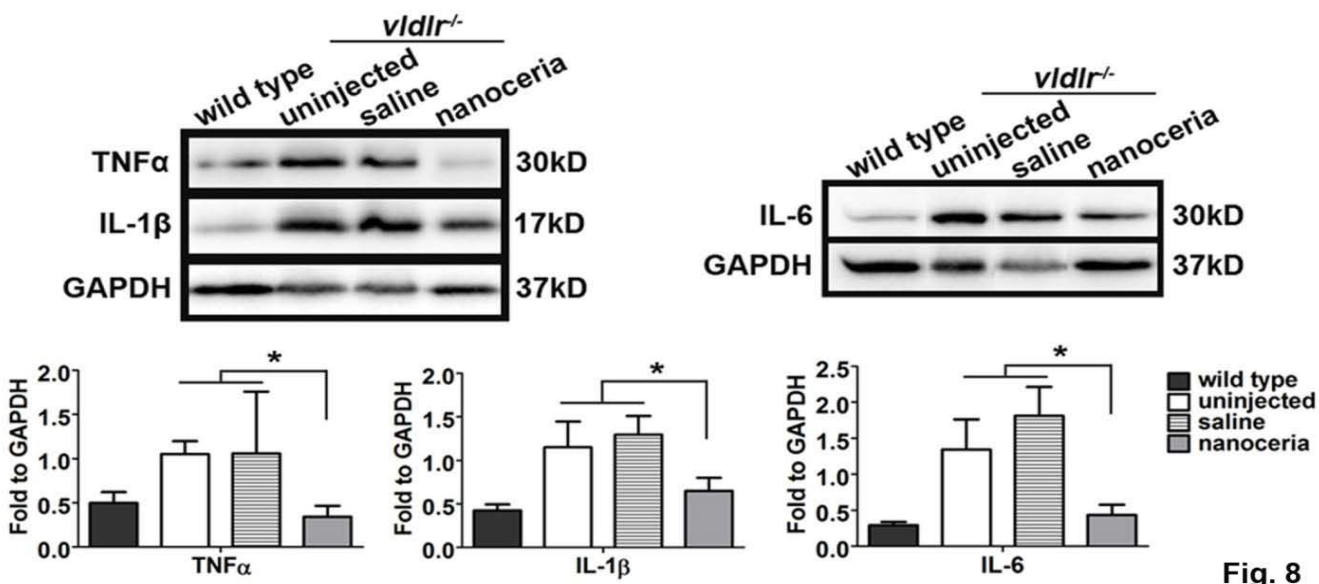


Fig. 8

Figure 8: Nanoceria down regulate major inflammatory cytokines. Western blots at P35d demonstrated that TNFα, IL-1β and IL-6 are greatly up regulated in the un.injected and saline treated eyes, whereas nanoceria treatment significantly reduced the levels of these cytokines. N=4-6 eyes per group. *P<0.05.

was similar in both wt and mutant at P35d, but at P7m the RPE cells in the mutant exhibited frequent discontinuities of the boundary and numerous damaged areas. Immunocytochemistry of cryosections at P35d and P7m demonstrated that the RPE65 fluorescence (Figure 7A) was weak and distributed in the swollen and irregular shaped RPE cells with some areas of discontinuity in the mutant mouse. The connections between the cells are loose, compared to the very

dense borders of intact and uniform shaped RPE cells in the wt controls. ZO-1 protein labeling (Figure 7B) in the mutant was weaker and showed discontinuity, compared to the more continuous and brighter fluorescence of ZO-1 labeling in wt. Nanoceria treatment greatly increased the fluorescence intensity of these two proteins in the mutant (Figure 7A & Figure B). Western blot assay at P35d and P7m indicated that un.injected *vldlr*^{-/-} mice have decreased levels of

RPE65 (Figure 7C), ZO-1 (Figure 7D) and Occludin (Figure 7E & Figure 7F), which are 2.5, 4.7, and 3.7 fold less, respectively, than those of wt. These decreases are indicative of breakdown/malfunction of the BRB and increased vascular permeability in *vldlr*^{-/-} mice. However, nanoceria treatment elevated these proteins to amounts equivalent to wt.

Nanoceria decrease the expression of pro-inflammatory cytokines

TNF- α is a principal inflammatory factor and was reported to be elevated and involved in the increased BRB permeability [28,29] and pathology of the *vldlr*^{-/-} phenotype [30]. To examine the expression of TNF- α , and other inflammatory factors in *vldlr*^{-/-} mice, western blot assays were carried out. As shown in Figure 8, TNF- α , IL-1 β and IL-6 were up-regulated 2.1, 2.7 and 4.6 fold respectively, in the uninjected and saline injected mice compared to the wt, whereas nanoceria treatment significantly decreased their expression to that of wt.

Discussion

The physicochemical properties of nanoparticles determine their function. Specifically, the size and surface charge of the nanoparticles play critical roles in their cellular uptake, internalization, localization, free radical scavenging and even toxicity [27,31,32]. Surface charge of the particles also determines their attachment and binding to the membrane (which has negatively charged domains) and subsequent internalization [33]. It has been shown that nanoceria, at a concentration below 1 mM, exhibit a variable surface charge but a positive charge remained on the surface when concentrations were above 1 mM [27]. Here we showed that nanoceria decreased the level of VEGF expression and reduced the number of RNV and CNV in a dose-dependent manner. Although nanoceria at 1 μ M produced positive effects, the most effective dose was 1mM, and the highest dose we tested (10 mM) was no more effective than the 1 μ M dose. These results further confirmed the conclusion that injection of 1 μ l of 1 mM is optimal for producing the highest therapeutic effect *in vivo* [27]. We have shown that 1 μ l of nanoceria at 10 mM does not have an adverse effect on retinal structure and function, and does not cause an acute or chronic increase in inflammatory cytokines in wt mice [25]. As with many therapeutic agents, too much of a good thing is bad, or in this case simply less effective.

RPE cells are essential structural and physiological components needed for the regeneration of the visual pigment and they also phagocytose the aged discs of outer segments of the rods and cones which enables renewal of the photoreceptor outer segments [2,34]. Accumulated evidence suggests that loss of RPE function precedes the death of photoreceptors in AMD [15]. The RPE cells form the outer BRB that is critical for controlling the precise movement and exchange of molecules and nutrients between the choroid and the retina [1,3,4]. The tight junction is an integral component of the primary structure that enables the BRB to prevent subretinal edema. It has been reported that oxidative stress, caused by light exposure [35] or hydrogen peroxide [36], disrupts the cell-cell junctional structures and immunostaining patterns of ZO-1, N-cadherin and β -catenin in Balb/C mice and in RPE19 cells. Decreased expression of ZO-1 [30,37] or Occludin [6] and the consequent breakdown of the BRB and increased vascular permeability have been reported in *vldlr*^{-/-} mice, diabetic retinopathy and ischemia mice. Furthermore,

knockdown of ZO-1 resulted in the loss of the polarization and changed the morphology of RPE cells, implying dysfunction of the RPE [38]. In the current study, we show that albino *vldlr*^{-/-} mice have RPE cells without RPE65 protein in their cytoplasm, and the labeling of the tight junction protein adaptor, ZO-1, was observed to be disrupted compared to its very uniform and continuous boundaries in wt mice. In addition, the RPE cells in the immunostained cryosections from the mutant mice were shown to have irregular-shapes. The localization patterns of both RPE65 and ZO-1 were altered with much weaker staining compared to the regular and intense signals seen in wt, suggesting decreased amounts and distributions of RPE65 and ZO-1 in the RPE cells.

Western blot assays further demonstrated that the levels of RPE65 and junctional complex proteins (ZO-1 and Occludin) are greatly decreased in the untreated mutant mice, reflecting the BRB breakdown/malfunction and dysregulation of vascular permeability in *vldlr*^{-/-} mice. This phenomenon was further demonstrated by fluorescein angiographic evaluation of the time course of fluorescein leakage in the *vldlr*^{-/-} mice. Collectively, these findings, in agreement with those of Chen and colleagues [30], support the conclusion that the BRB is impaired in *vldlr*^{-/-} mice. However, antioxidant nanoceria treatment significantly increased the amount of RPE65 and junctional proteins and inhibited the fluid leakage, suggesting that nanoceria, by destroying the excessive ROS, maintain normal RPE integrity and function, and thereby prevent increased permeability of the BRB.

Inflammatory cytokines play an important role in development of AMD and pathological neovascularization, disruption of the BRB morphology and function, increases in vascular permeability and RPE-choroid changes [28,35,39,40]. The phenotype and pathology of the *vldlr*^{-/-} mouse have been shown to be correlated with chronic inflammation [30] through up-regulation of TNF α , NF- κ B and subsequently VEGF [41]. IL-1 β has been shown to promote neovascularization in laser injured C57BL/6j and Cx3cr1^{-/-} mice and light injured albino mice [42], and recently, it was identified as an important effector of inflammasome (NLRP3) activation, which has been implicated in AMD pathogenesis [43,44]. The excessive levels of VEGF [30,45,46] were demonstrated to promote the development of abnormal blood vessels rather than regulate normal vascular development, and inhibition of VEGF has served as a therapeutic strategy for treatment of AMD and neovascular diseases [41,47,48]. It has been shown that elevation of VEGF expression is closely related with disruption of the tight junction complex and breakdown of the BRB which consequently results in increased vascular permeability [9-10,49]. Our previous PCR array analyses showed that nanoceria inhibit expression of genes associated with inflammation and angiogenesis within one week [50]. In the current study, data obtained from western blots show that VEGF is elevated in *vldlr*^{-/-} mice when examined at P35d and P7m. Pro-inflammatory cytokines, TNF- α , IL-1 β and IL-6 are also elevated in the mutant retinas, and nanoceria treatment decreases their expression. In our earlier report on the pigmented *vldlr*^{-/-}, we demonstrated that nanoceria act as direct antioxidants and function similar to Thioredoxin (Trx) to down regulate the level of VEGF and inhibit/regress neovascularization through regulation of the ASK1-P38/JNK-NF- κ B signaling pathway [23]. Our current report further demonstrates that nanoceria, by modulation of inflammatory cytokines; protect the RPE against

oxidative stress-induced damage and the loss of BRB function.

Conclusion

Our data demonstrated that nanoceria decrease the expression of VEGF and the number of retinal and choroidal neovascularization in a dose-dependent manner following a single intravitreal injection, with 1 μ l of 1 mM (172 ng) producing the maximum effect. Nanoceria also up regulate RPE65 and the components of the RPE junctional complex, regress neovascularization, inhibit vascular permeability, and down regulate pro-inflammatory cytokines.

Acknowledgement

The authors thank the personnel at the animal, imaging and molecular modules of the Vision Research Core Facility at the Oklahoma University Health Sciences Center.

Financial Support

This work was supported in part by National Institutes of Health (NIH) National Eye Institute (NEI) P30 EY021725, R21EY018306, R01EY018724 and R01EY022111, National Science Foundation: CBET-0708172 and unrestricted funds from RPB.

Disclosure Statement

Cai X, none. Seal S and McGinnis JF are listed as inventors in patents.

References

- Runkle EA, Antonetti DA. The blood-retinal barrier: structure and functional significance. *Methods Mol Biol.* 2011; 686: 133-48.
- Strauss O. The retinal pigment epithelium in visual function. *Physiol Rev.* 2005; 85: 845-881.
- Campbell M, Humphries P. The blood-retina barrier: tight junctions and barrier modulation. *Adv Exp Med Biol.* 2012; 763: 70-84.
- Rizzolo LJ, Peng S, Luo Y, Xiao W. Integration of tight junctions and claudins with the barrier functions of the retinal pigment epithelium. *Prog Retin Eye Res.* 2011; 30: 296-323.
- Gonzalez-Mariscal L, Betanzos A, Nava P, Jaramillo BE. Tight junction proteins. *Prog Biophys Mol Biol.* 2003; 81: 1-44.
- Xu HZ, Le YZ. Significance of outer blood-retina barrier breakdown in diabetes and ischemia. *Invest Ophthalmol Vis Sci.* 2011; 52: 2160-2164.
- Xu HZ, Song Z, Fu S, Zhu M, Le YZ. RPE barrier breakdown in diabetic retinopathy: seeing is believing. *J Ocul Biol Dis Infor.* 2011; 4: 83-92.
- Erickson KK, Sundstrom JM, Antonetti DA. Vascular permeability in ocular disease and the role of tight junctions. *Angiogenesis.* 2007; 10: 103-117.
- Vinores SA, Seo MS, Okamoto N, Ash JD, Wawrousek EF, Xiao WH, et al. Experimental models of growth factor-mediated angiogenesis and blood-retinal barrier breakdown. *Gen Pharmacol.* 2000; 35: 233-239.
- Vinores SA. Breakdown of the blood-retinal barrier. *Immunology, Inflammation and Diseases of the Eye.* 2011: 300-306.
- Cai X, McGinnis JF. Oxidative stress: the achilles' heel of neurodegenerative diseases of the retina. *Front Biosci.* 2012; 17: 1976-1995.
- Hollyfield JG, Bonilha VL, Rayborn ME, Yang X, Shadrach KG, Lu L, et al. Oxidative damage-induced inflammation initiates age-related macular degeneration. *Nat Med.* 2008; 14: 194-198.
- Ambati J, Fowler BJ. Mechanisms of age-related macular degeneration. *Neuron.* 2012; 75: 26-39.
- Bowes Rickman C, Farsiu S, Toth CA, Klingeborn M. Dry age-related macular degeneration: mechanisms, therapeutic targets, and imaging. *Invest Ophthalmol Vis Sci.* 2013; 54: 68-80.
- Kinnunen K, Petrovski G, Moe MC, Berta A, Kaamiranta K. Molecular mechanisms of retinal pigment epithelium damage and development of age-related macular degeneration. *Acta Ophthalmol.* 2012; 90: 299-309.
- Karakoti AS, Monteiro-Riviere NA, Aggarwal R, Davis JP, Narayan RJ, Self WT, et al. Nanoceria as Antioxidant: Synthesis and Biomedical Applications. *JOM.* 2008; 60: 33-37.
- Pirmohamed T, Dowding JM, Singh S, Wasserman B, Heckert E, Karakoti AS, et al. Nanoceria exhibit redox state-dependent catalase mimetic activity. *Chem Commun (Camb).* 2010; 46: 2736-2738.
- Korsvik C, Patil S, Seal S, Self WT. Superoxide dismutase mimetic properties exhibited by vacancy engineered ceria nanoparticles. *Chem Commun (Camb).* 2007; 10: 1056-1058.
- Chen J, Patil S, Seal S, McGinnis JF. Rare earth nanoparticles prevent retinal degeneration induced by intracellular peroxides. *Nat Nanotechnol.* 2006; 1: 142-150.
- Cai X, Sezate SA, Seal S, McGinnis JF. Sustained protection against photoreceptor degeneration in tubby mice by intravitreal injection of nanoceria. *Biomaterials.* 2012; 33: 8771-8781.
- Kong L, Cai X, Zhou X, Wong LL, Karakoti AS, Seal S, et al. Nanoceria extend photoreceptor cell lifespan in tubby mice by modulation of apoptosis/survival signaling pathways. *Neurobiol Dis.* 2011; 42: 514-523.
- Zhou X, Wong LL, Karakoti AS, Seal S, McGinnis JF. Nanoceria inhibit the development and promote the regression of pathologic retinal neovascularization in the Vldlr knockout mouse. *PLoS One.* 2011; 6: 16733.
- Cai X, Seal S, McGinnis JF. Sustained inhibition of neovascularization in vldlr^{-/-} mice following intravitreal injection of cerium oxide nanoparticles and the role of the ASK1-P38/JNK-NF- κ B pathway. *Biomaterials.* 2014; 35: 249-258.
- Wong LL, Hirst SM, Pye QN, Reilly CM, Seal S, McGinnis JF. Catalytic nanoceria are preferentially retained in the rat retina and are not cytotoxic after intravitreal injection. *PLoS One.* 2013; 8: 58431.
- Cai X, Seal S, McGinnis JF. Non-toxic retention of nanoceria in murine eyes. *Mol Vis.* 2016; 22: 1176-1187.
- Hu W, Jiang A, Liang J, Meng H, Chang B, Gao H, et al. Expression of VLDLR in the retina and evolution of subretinal neovascularization in the knockout mouse model's retinal angiomas proliferation. *Invest Ophthalmol Vis Sci.* 2008; 49: 407-415.
- Vincent A, Inerbaev TM, Babu S, Karakoti AS, Self WT, Masunov AE, et al. Tuning hydrated nanoceria surfaces: experimental/theoretical investigations of ion exchange and implications in organic and inorganic interactions. *Langmuir.* 2010; 26: 7188-7198.
- Shirasawa M, Sonoda S, Terasaki H, Arimura N, Otsuka H, Yamashita T, et al. TNF- α disrupts morphologic and functional barrier properties of polarized retinal pigment epithelium. *Exp Eye Res.* 2013; 110: 59-69.
- Aveleira CA, Lin CM, Abcouwer SF, Ambrosio AF, Antonetti DA. TNF- α signals through PKC ζ /NF- κ B to alter the tight junction complex and increase retinal endothelial cell permeability. *Diabetes.* 2010; 59: 2872-2882.
- Chen Y, Hu Y, Moiseyev G, Zhou KK, Chen D, Ma JX. Photoreceptor degeneration and retinal inflammation induced by very low-density lipoprotein receptor deficiency. *Microvasc Res.* 2009; 78: 119-127.
- Patil S, Sandberg A, Heckert E, Self W, Seal S. Protein adsorption and cellular uptake of cerium oxide nanoparticles as a function of zeta potential. *Biomaterials.* 2007; 28: 4600-4607.
- Vincent A, Babu S, Heckert E, Dowding J, Hirst SM, Inerbaev TM, et al. Protonated nanoparticle surface governing ligand tethering and cellular targeting. *ACS Nano.* 2009; 3: 1203-1211.
- Cai X, Seal S, McGinnis JM. Cerium oxide nanoparticle reduction of oxidative damage in retina. *Springer.* 2012; 399-418.

34. Cai X, Conley SM, Naash MI. RPE65: role in the visual cycle, human retinal disease, and gene therapy. *Ophthalmic Genet.* 2009; 30: 57-62.
35. Narimatsu T, Ozawa Y, Miyake S, Kubota S, Hirasawa M, Nagai N, et al. Disruption of cell-cell junctions and induction of pathological cytokines in the retinal pigment epithelium of light-exposed mice. *Invest Ophthalmol Vis Sci.* 2013; 54: 4555-4562.
36. Bailey TA, Kanuga N, Romero IA, Greenwood J, Luthert PJ, Cheetham ME. Oxidative stress affects the junctional integrity of retinal pigment epithelial cells. *Invest Ophthalmol Vis Sci.* 2004; 45: 675-684.
37. Leal EC, Manivannan A, Hosoya K, Terasaki T, Cunha-Vaz J, Ambrosio AF, et al. Inducible nitric oxide synthase isoform is a key mediator of leukostasis and blood-retinal barrier breakdown in diabetic retinopathy. *Invest Ophthalmol Vis Sci.* 2007; 48: 5257-5265.
38. Georgiadis A, Tschernutter M, Bainbridge JW, Balaggan KS, Mowat F, West EL, et al. The tight junction associated signalling proteins ZO-1 and ZONAB regulate retinal pigment epithelium homeostasis in mice. *PLoS One.* 2010; 5: 15730.
39. Ambati J, Atkinson JP, Gelfand BD. Immunology of age-related macular degeneration. *Nat Rev Immunol.* 2013; 13: 438-451.
40. Chen M, Xu H. Parainflammation, chronic inflammation, and age-related macular degeneration. *J Leukoc Biol.* 2015; 98: 713-725.
41. Chen Y, Hu Y, Lu K, Flannery JG, Ma JX. Very low density lipoprotein receptor, a negative regulator of the wnt signaling pathway and choroidal neovascularization. *J Biol Chem.* 2007; 282: 34420-34428.
42. Lavalette S, Raoul W, Houssier M, Camelo S, Levy O, Calippe B, et al. Interleukin-1 β inhibition prevents choroidal neovascularization and does not exacerbate photoreceptor degeneration. *Am J Pathol.* 2011; 178: 2416-2423.
43. Marneros AG. NLRP3 inflammasome blockade inhibits VEGF-A-induced age-related macular degeneration. *Cell Rep.* 2013; 4: 945-958.
44. Tseng WA, Thein T, Kinnunen K, Lashkari K, Gregory MS, D'Amore PA, et al. NLRP3 inflammasome activation in retinal pigment epithelial cells by lysosomal destabilization: implications for age-related macular degeneration. *Invest Ophthalmol Vis Sci.* 2013; 54: 110-120.
45. Dorrell MI, Aguilar E, Jacobson R, Yanes O, Gariano R, Heckenlively J, et al. Antioxidant or neurotrophic factor treatment preserves function in a mouse model of neovascularization-associated oxidative stress. *J Clin Invest.* 2009; 119: 611-623.
46. Penn JS, Madan A, Caldwell RB, Bartoli M, Caldwell RW, Hartnett ME. Vascular endothelial growth factor in eye disease. *Prog Retin Eye Res.* 2008; 27: 331-371.
47. Gu L, Chen H, Tuo J, Gao X, Chen L. Inhibition of experimental choroidal neovascularization in mice by anti-VEGFA/VEGFR2 or non-specific siRNA. *Exp Eye Res.* 2010; 91: 433-439.
48. Wang Y, Wang VM, Chan CC. The role of anti-inflammatory agents in age-related macular degeneration (AMD) treatment. *Eye (Lond).* 2011; 25: 127-139.
49. Antonetti DA, Barber AJ, Khin S, Lieth E, Tarbell JM, Gardner TW. Vascular permeability in experimental diabetes is associated with reduced endothelial occludin content: vascular endothelial growth factor decreases occludin in retinal endothelial cells. *Penn State Retina Research Group. Diabetes.* 1998; 47: 1953-1959.
50. Kyosseva SV, Chen L, Seal S, McGinnis JF. Nanoceria inhibit expression of genes associated with inflammation and angiogenesis in the retina of Vldlr null mice. *Exp Eye Res.* 2013; 116: 63-74.